Improving Vehicle Stability and Comfort through Active Corner Positioning

Skrickij, Viktor; Šabanovič, Eldar; Kojis, Paulius; Zuraulis, Vidas; Ivanov, Valentin; Shyrokau, Barys

DOI
10.4271/2024-01-2552

Publication date
2024

Document Version
Final published version

Published in
SAE Technical Papers

2024-01-2552 Published 09 Apr 2024

Improving Vehicle Stability and Comfort through Active Corner Positioning

Viktor Skrickij, Eldar Šabanovič, Paulius Kojis, and Vidas Žuraulis Vilnius Gediminas Technical University

Valentin Ivanov Technische Universitat Ilmenau

Barys Shyrokau Delft Univ of Technology

Citation: Skrickij, V., Šabanovič, E., Kojis, P., Žuraulis, V. et al., "Improving Vehicle Stability and Comfort through Active Corner Positioning," SAE Technical Paper 2024-01-2552, 2024, doi:10.4271/2024-01-2552.

Received: 16 Oct 2023 Revised: 26 Dec 2023 Accepted: 18 Jan 2024

Abstract

The emergence of new electric vehicle (EV) corner concepts with in-wheel motors offers numerous opportunities to improve handling, comfort, and stability. This study investigates the potential of controlling the vehicle's corner positioning by changing wheel toe and camber angles. A high-fidelity simulation environment was used to evaluate the proposed solution. The effects of the placement of the corresponding actuators and the actuation point on the force required during cornering were investigated. The results demonstrate that the toe angle, compared to the camber angle, offers more effect for improving the vehicle dynamics. The developed direct yaw rate control with four toe actuators improves stability, has a positive effect on comfort, and contributes to the development of new active corner architectures for electric and automated vehicles.

Introduction

The automotive industry is facing challenging and inspiring developments in terms of new sustainable vehicle concepts and automation. The elimination of the internal combustion engine requires the development of new powertrain solutions, with a focus on electrification. A variant, where electrification enables a redesign of vehicle architecture, is the integration of in-wheel motors (IWMs) as part of an active corner solution. Vehicles equipped with IWMs demonstrate significantly improved propulsion and braking capabilities while increasing stability and optimizing power consumption, bringing further benefits to handling, stability and comfort improvement [1].

The handling and comfort features of EVs are becoming increasingly important in the case of automated mobility. This is due to the fact that passengers have the opportunity to engage in various activities during their journey, such as working on a laptop or reading a book [2]. Achieving a ride comfort akin to that of a train journey is highly desirable to ensure passenger comfort in vehicles [3]. To improve the comfort of the occupants, different solutions can be used. One such approach is to use light alloy and carbon fiber parts to reduce the unsprung masses; however, with an IWM, the unsprung masses remain higher than for the conventional vehicle design [4]. Therefore, additional engineering solutions for corners are required. So far, the most analyzed solution has been semi-active and active suspension systems [5, 6]. This solution can be adopted without significant modifications in vehicle design, and together can significantly improve both handling and comfort. Several semi/active suspension control solutions have been developed so far for vehicles with IWMs [7, 8, 9]. In all these studies only objective metrics have been used for vehicle dynamics evaluation. It is a limiting factor as subjective measures remain an essential aspect of comfort assessment [10]. As subjective studies cannot be applied in the simulation environment, the solution could be the adaptation of difference thresholds (DTs) - the minimum change in the magnitude of the whole-body vibration required for the occupant to perceive the change in magnitude [11].

This paper investigates the new design of EVs with active corner positioning to improve stability and comfort. Active corner positioning includes control of toe and camber angles, assessment is performed using both objective metrics and DT. The next sections of the paper include (II) a brief analysis of the state of the art, (III) the impact of toe and camber angles on vehicle dynamics and identification of the most preferred design, (IV) a vehicle model for defining reference parameters used for control, development of the controller for active corner positioning, and (V) the results of a simulation study demonstrating the operation of the active corner.

Related Works

Despite the widespread opinion that increased unsprung mass will have adverse effects on vehicle dynamics, experimental investigations showed that the effects are not as significant as expected [12]. The results obtained have shown the benefits of IWMs by improving most of the vehicle performance criteria and corners may become an essential part of the next generation of electric vehicles. As the current ride comfort level of a conventional vehicle is not enough [2], additional measures for ride comfort improvement need to be taken into account while designing EVs with corners [13].

Wheel corner modules may incorporate semi/active damping and wheel positioning actuators. This way stability and comfort are enhanced and wheel toe, camber angles are adjusted actively while driving [14, 15]. The approach is based on the fact that the magnitude of the tire lateral force depends on the wheel slip and camber angles, vertical load, tire inflation pressure, and mechanical properties of the tire [16]. When the tire has no slip angle, the lateral force generated depends solely on the camber angle of the wheels, called camber thrust. Camber angle varies with suspension travel, steering wheel angle, and rubber bushing deformation [17]. The toe angle is expressed as the difference between the values of vehicle track width measured at the inner and outer edges of the tire. The value of static toe angle depends on various vehicle suspension characteristics: Ackermann or inverse Ackermann geometry, steering, roll behavior, compliance, and camber angle. Toe angle affects three main characteristics: tire wear, straight-line stability, and vehicle controllability during cornering [15]. Wheel camber and toe angles are presented in the Figure 1.

FIGURE 1 Wheel camber and toe angles

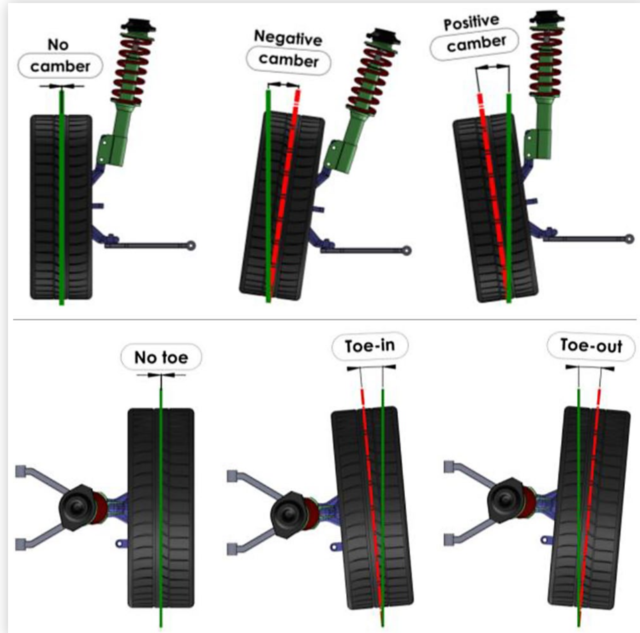

Various solutions exist for active wheel positioning. One notable approach is outlined in [18]. It introduces a rule-based camber control strategy. This strategy employs the steering angle as an input for camber control, while also considering lateral acceleration as a primary factor. The study reveals that increasing the camber angle of the wheels during higher lateral acceleration scenarios can lead to a reduction in energy consumption. In the pursuit of enhancing vehicle path tracking and yaw stability, another innovative system, detailed in [19], introduces an active camber control system. This system operates within the framework of model predictive control (MPC) and employs a simulation environment that utilizes a planar vehicle model and a modified Dugoff tire model. The results demonstrate a 9% increase in vehicle passing speed, coupled with improved tire friction utilization and reduced path tracking errors during double lane change (DLC) maneuver. Furthermore, the exploration of dynamic camber and toe control, as presented in [20], involves the use of a proportional integral derivative (PID) controller. Such an approach effectively reduces the vertical acceleration of the sprung mass, as an objective metric root mean square (RMS) value is used. RMS of vertical acceleration serves as a crucial metric for defining ride comfort. Finally, rear axle toe control, a common technique in rear-wheel steering, emerges as a significant contributor to enhancing a vehicle's lateral and yaw motion, as highlighted in [21]. A variety of actuators have been designed for wheel positioning control. They can be categorized based on their functionality, with central placement employing one actuator per axis and dual featuring a separate actuator for each wheel on the axis. In terms of operational principles, these actuators can be either electric, such as the solutions offered by ZF, or hydraulic, as proposed by Bosch. In summary, these various approaches showcase the diverse strategies employed in the realm of active wheel positioning, each offering unique advantages and insights into improving vehicle performance and comfort.

The objective of this study was to determine the required specifications for the actuators and to analyze the potential benefits of active control of camber and toe angles for vehicle dynamics. At the beginning, the CAD design of the corner architecture and the possibility of incorporating actuators are analyzed. Then, the simulations were performed to determine the effects of camber and toe changes focusing on assessment of vehicle comfort, and stability. Thorough evaluation of the active corner positioning system using both objective metrics and DTs has been performed. This combined assessment approach provides a more holistic understanding of the system's performance and its impact on the user's experience. Finally, a control strategy for the selected wheel positioning technology was developed and tested in a simulation environment.

Main contributions of this work are:

- New corner design is proposed and pathways for active wheel positioning have been defined.
- Enhanced control strategy for active corner positioning is designed to improve the performance of the active corner positioning system.

The Concept of Corner Positioning

To improve vehicle dynamics, the influence of toe and camber angles is analyzed. The location of the actuation point and the wheel pivot point (Figure 2) plays a crucial role in determining the force required for the system to function properly. This force requirement corresponds to the load on the chassis and body connection points; in addition, large actuation forces cause increased energy consumption. The multibody simulation analysis for camber angle variation has shown that the pivot point at the tire contact patch (Figure 2 a) is less affected by the vertical motion of the wheel, allowing wider camber and toe adjustment. In this case, a smaller actuation force is required [22]. In contrast, the pivot point on an axis plane (Figure 2 b) requires more space for the actuator and a higher actuation force.

Due to suspension kinematics and compliance, toe, camber angle, and track are being changed as the wheel moves vertically. This should be considered when developing corner designs and mathematical models for simulations. SUV vehicle was selected as a reference and new corners were designed. Main vehicle parameters are provided in Table 1. The suspension of the selected vehicle features a relatively simple design and high efficiency.

FIGURE 2 Wheel pivot point position (shown by red dot): a) wheel road contact point; b) wheel hub center point

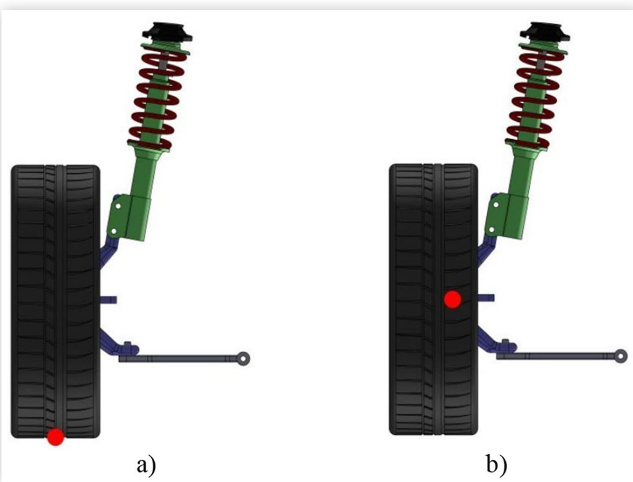

TABLE 1 Vehicle parameters

Wheelbase	2.675 m
Distance between front axle and COG	1.439 m
Distance between rear axle and COG	1.236 m
Height of COG above ground	0.65 m
Track width	1.625 m
Vehicle mass	2302 kg
Total unsprung mass	285 kg
Tire size	235/55/R19
Yaw inertia	3231 kgm^2

FIGURE 3 Designed SUV (a) front and (b) rear corners with IWMs

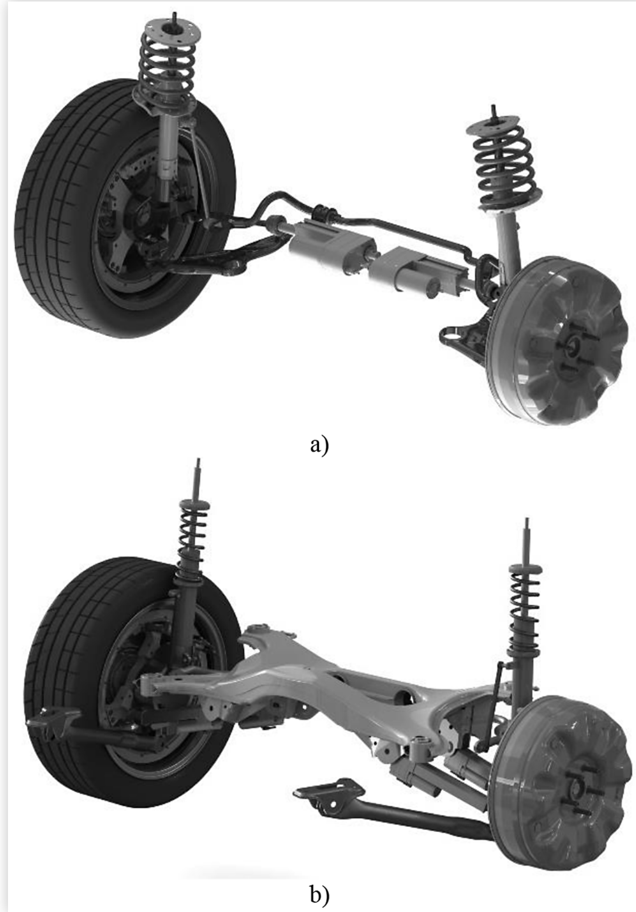

The new design of the front and rear corners is shown in Figure 3. The new design increases unsprung mass by 48% at the front corners and 46% at the rear corners. The use of lightweight solutions reduced the masses by 14% and 9%, respectively. However, reducing the mass to the initial values (compared to a conventional powertrain) is insufficient and requires a high level of effort [4].

To explore the performance of SUV vehicle, a high-fidelity model with new corners and an experimentally validated FTire tire model was created in MSC Adams Car [23]. The results of the parallel wheel travel test are shown in Figure 4. The outcome of these tests were kinematics and compliance look-up tables which later are incorporated into high-fidelity vehicle models realized in IPG Carmaker software.

A. Camber and Toe Impact on Vehicle Dynamics

Simulations were performed to capture the working force moments, with the camber actuator experiencing an overturning moment Mx and the self-aligning moment Mz for the toe. All the properties of the original components were taken from the reference vehicle, while the properties of the modified and redesigned parts were

FIGURE 4 Impact of vertical wheel travel on the toe and camber angles: a) front corner; b) rear corner

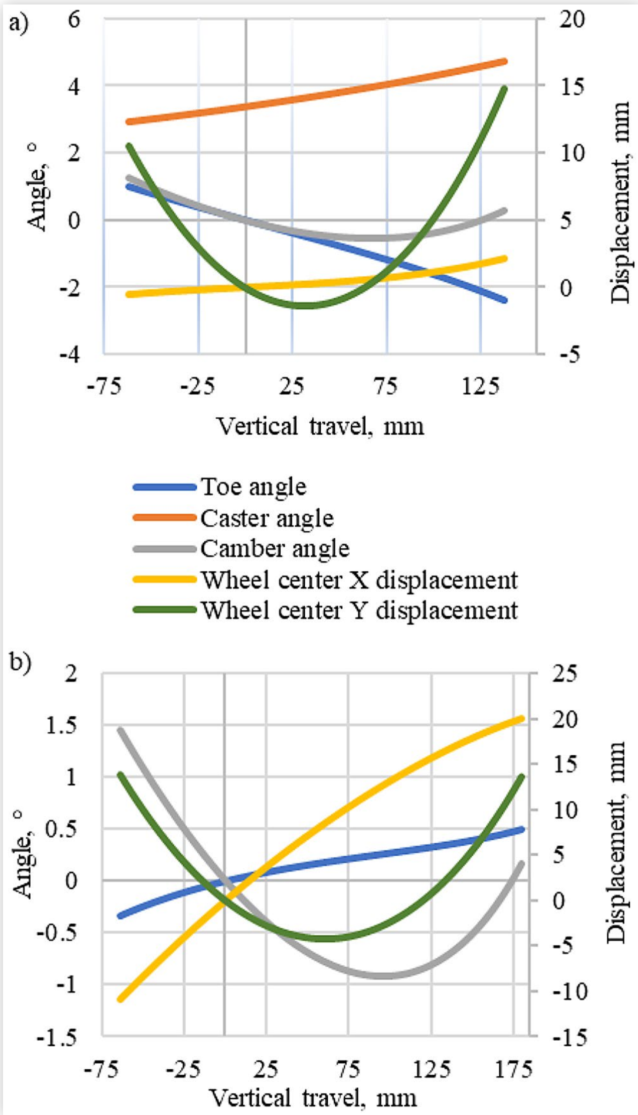

taken from the CAD models after topology optimization. Several test maneuvers, such as Sine with Dwell, single and DLC, constant radius cornering, fish-hook and riding on rough roads, were performed at different speeds to define the loads that the actuators must produce.

The simulations showed that the maximum moment around the X-axis was 353 Nm and the camber actuator was positioned at the upper mount of the damper, resulting in a height of 1031 mm. It follows that the minimum force for the camber actuator is 343 N. However, such an actuator arrangement would require significant changes to the vehicle design. The total actuator travel required to achieve camber changes in the interval [-6°, +6°] is 220 mm. Further increasing the camber angle would require the use of a tire with a rounded shape to reduce wear and provide a better grip. If the same wheel pivot point is chosen, the height on which the toe actuator force acts is between 91 and 103 mm. From the simulations, the highest value of the M_z moment is 182 Nm. This results in a total actuating force of 2000 N. The requirements for the toe actuator travel results from the kinematics of the wheel suspension and should be around 100 mm, while using with camber actuator. If only toe actuators are used the displacement is decreased to around 20 mm

According to the simulations performed, the toe control showed more promising results compared to the camber angle control. Camber variation produced roll increase, and as a result the largest RMS of sideslip angle, lateral acceleration and tire lateral forces. Varying the toe angle is much more effective than the camber; it does not require significant changes to the vehicle and can be controlled over a wide range with conventional tires, while the camber angle can only be adjusted over a range of [-6°, +6°].

B. Vehicle with Active Toe Positioning

This subsection introduces the overall wheel positioning control system architecture and provides governing equations. Figure 5 presents a simplified outline of the control structure. The reference yaw rate is calculated by considering the measured road wheel angles on both the front and rear axles, as well as estimates of vehicle speed and the maximum friction coefficient.

The bicycle vehicle model (Figure 6) was used to develop wheel positioning control.

For conventional vehicles, the dependence on front-wheel steering can be expressed as follows [24]:

$$\delta = \frac{l}{R} + \left(\frac{ml_r}{C_{\alpha f} l} - \frac{ml_f}{C_{\alpha r} l} \right) \frac{V^2}{R}; \tag{1}$$

FIGURE 5 Simplified controller structure

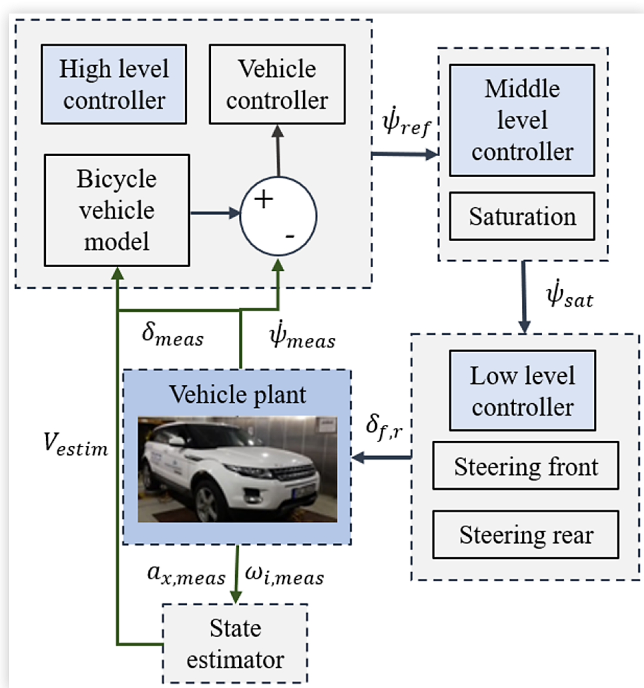

FIGURE 6 Bicycle model for 4-wheel steering vehicle

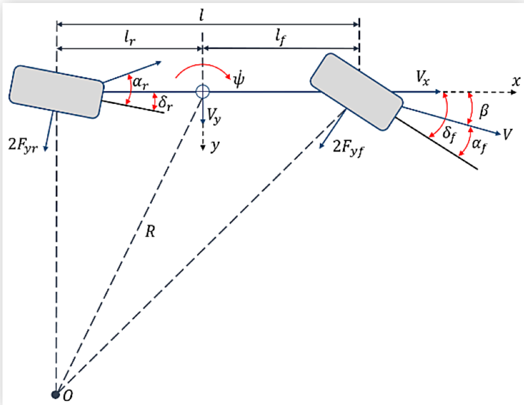

where l – vehicle base [m]; R – trajectory radius [m]; m – vehicle mass [kg]; $l_{f,r}$ – distance from the center of gravity to the front/rear axle [m]; $C_{\alpha f,r}$–tire cornering stiffness for front and rear axle [N/rad]; V- vehicle velocity [m/s].

Eq. (1) can be rewritten as

$$\delta = \left(\frac{l}{V} + K_{us}V\right)\psi; \tag{2}$$

where K_{us} – understeer gradient [$rad \cdot s^2/m$]; ψ – yaw rate [rad/s].

In the case of the toe control, the steering effect takes place on both the front and rear axles. In such a case, Eq. (2) can be rewritten [24]:

$$\delta = \delta_f - \delta_r = \left(\frac{l}{V} + K_{us}V\right)\psi. \tag{3}$$

Structurally, steering is implemented by four additional toe actuators on each wheel. With such an architecture, vehicle control can be improved. A reference yaw rate for a steady-state case is calculated from (3):

$$\psi_{ref} = \frac{V}{l + K_{us}V^2}\left(\delta_f - \delta_r\right); \tag{4}$$

The estimated (available) friction is needed to constrain the desired steady-state response, which can be selected based on the friction utilized. The maximum reference yaw rate can be determined as follows [25]:

$$\psi_{max} \approx 0.85\frac{\mu g}{V}; \tag{5}$$

where μ is the maximal friction coefficient, which can be estimated through different techniques, for example, using deep neural networks and computer vision, as shown in [26]. The saturated reference yaw rate is described:

$$\psi_{sat} = \begin{cases} \psi_{ref}, \left|\psi_{ref}\right| \le \psi_{max} \\ \pm\psi_{max}, \left|\psi_{ref}\right| > \psi_{max} \end{cases}. \tag{6}$$

The saturated steady-state response cannot describe the dynamic behavior of the vehicle. Therefore, the second-order transfer function can be used for this purpose:

$$\psi_{ref,d} = \frac{w_0^2\left(1+\tau s\right)}{s^2 + 2\xi w_0 s + w_0^2}\psi_{sat}; \tag{7}$$

where w_0 – natural frequency; and ξ – damping ratio. Yaw rate error is defined as:

$$\psi_{error} = \psi_{ref,d} - \psi_{actual}; \tag{8}$$

where ψ_{actual} is the actual yaw rate of the vehicle. When ψ_{error} increases up to the threshold, the yaw rate control is activated.

The positioning of the rear wheel can be implemented by proportional control, as shown in [23]:

$$\delta_r = k\left(V\right)\delta_f\left(t\right); \tag{9}$$

where $k(V)$ is a velocity-dependent proportional rear-wheel steering gain according to the front-wheel steering. In existing solutions for vehicles with a 4-wheel steering, the steering logic depends on the vehicle speed: at speeds below 40-60 km/h, the rear wheel is turned in the opposite direction to the front wheel (better maneuverability achieved); at speeds above 60 km/h, the wheels are turned in the same direction (better handling and stability) [24]. In this paper $k(V)$ was developed using the methodology presented in [24], it is presented in Figure 7.

The requirements for the controller were determined by the industry's need for low computational power and high robustness. PI control was proposed:

$$\Delta\delta_f = K_p\psi_{error} + K_i\int_0^t \psi_{error}dt; \tag{10}$$

FIGURE 7 Velocity-dependent proportional rear-wheel steering gain according to vehicle velocity

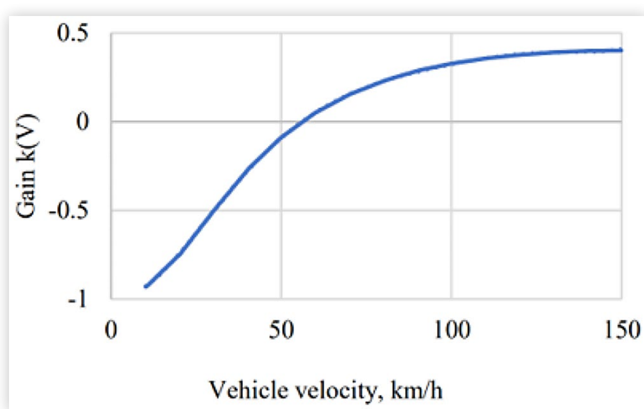

The proportional gain K_p is velocity-dependent gain and is calculated using Eqs. (4) and (9):

$$K_p = \frac{\psi_{error}\left(\frac{l}{V} + K_{us}V\right)}{\left(1 - k\left(V\right)\right)}. \tag{11}$$

Integral gain K_i is based on the integration of yaw rate error and it's magnitude.

Results

For the realization of the toe control for the front and rear axles as the most promising wheel positioning technique, a vehicle model was developed in IPG Carmaker, validated using field test data [27], modified according to the new corners design and combined with MATLAB/Simulink.

A. Positioning System Using Four Toe Actuators

Direct yaw rate control was implemented by using 4 toe actuators as part of the wheel positioning system. The Sine with Dwell (ISO 19365:2016) test was used to evaluate the proposed control system.

The vehicle speed is set to be 100 km/h, and the results are shown in Figure 8. It can be seen that the vehicle with passive corners is unstable during the indicated maneuver, and the yaw rate increases up to -1.06 rad/s.

It can be also observed that the yaw rate for the vehicle with the four wheels active toe control system switched on does not exceed -0.36 rad/s. Rear axle active toe control also helps to keep the vehicle stable during maneuver.

FIGURE 8 Vehicle yaw rate for the Sine with Dwell maneuver

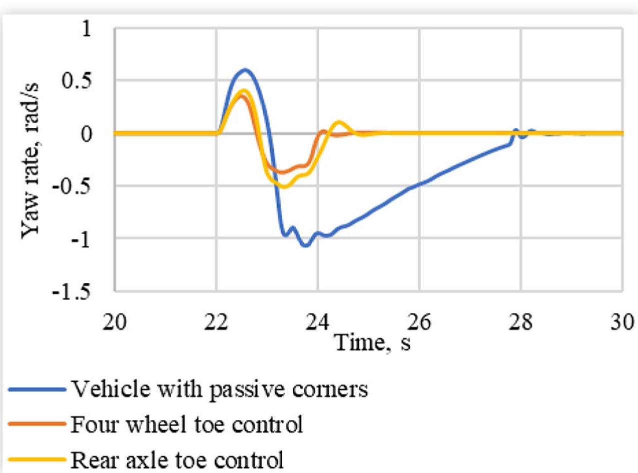

FIGURE 9 Vehicle trajectory (a) and velocity (b) for Sine with Dwell maneuver

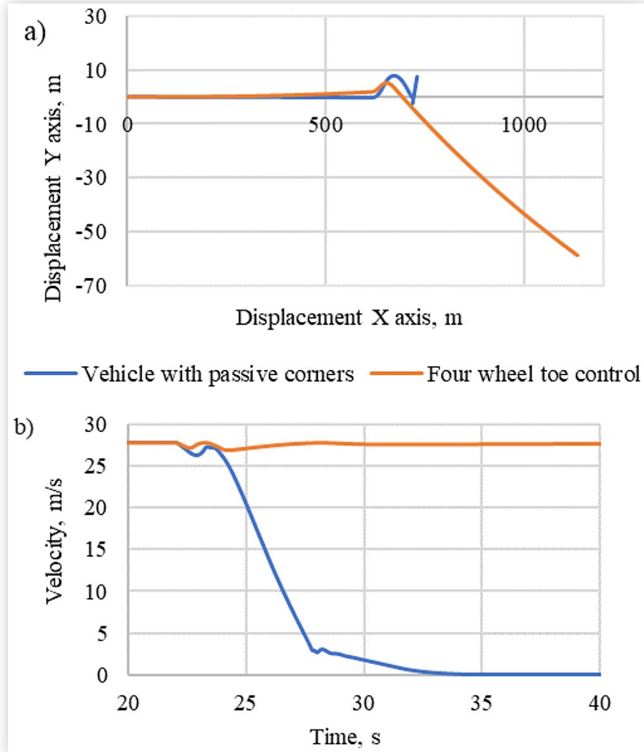

Furthermore, Figure 9 shows the trajectory and speed of the vehicle for the same maneuver. It can be seen that the vehicle with passive corners could not maintain the desired speed during the maneuver, while the vehicle with active corners could hold the required speed. Also, the passive corner based vehicle spins out at the end of the maneuver, hence there is such a significant difference in the trajectories (Figure 9a).

In addition, a simulation of DLC maneuver (ISO 3888-1:2018) was performed, its results are shown in (Figure 10). It can be observed that the vehicle with a passive corner design cannot perform a maneuver without exiting the barrier (Figure 10 b).

During a DLC maneuver vehicle speed was 80 km/h and the steering wheel input is following a predetermined sequence which is kept the same for both cases. As can be seen from Figure 10 (a) vehicle with passive corners achieved higher yaw rates compared to the vehicle with the active ones. In Figure 10 (b) vehicle trajectory is presented. The vehicle with passive corner design leaves the track in order to maintain the desired velocity. The proposed active toe control allows the vehicle to complete the maneuver within the road boundaries while maintaining the speed.

On the next step, the variations in sprung mass accelerations where investigated. In Figure 11, we present the initial results of the Sine with Dwell maneuver, revealing a noteworthy decrease in both lateral and vertical acceleration values. Specifically, the RMS for vertical acceleration, during the time span from 22 to 35 seconds, shifted from 0.46 m/s^2 to 0.20 m/s^2, marking a substantial 56.5%

FIGURE 10 Vehicle yaw rate for double lane-change maneuver: yaw rate (a) and trajectory (b)

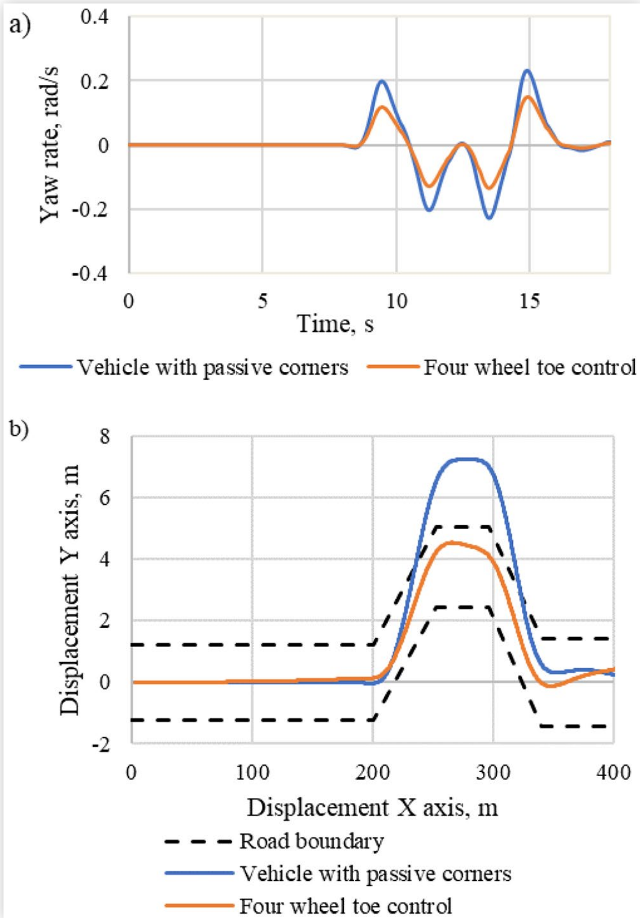

FIGURE 11 Accelerations achieved for Sine with Dwell test: lateral (a) and vertical acceleration (b)

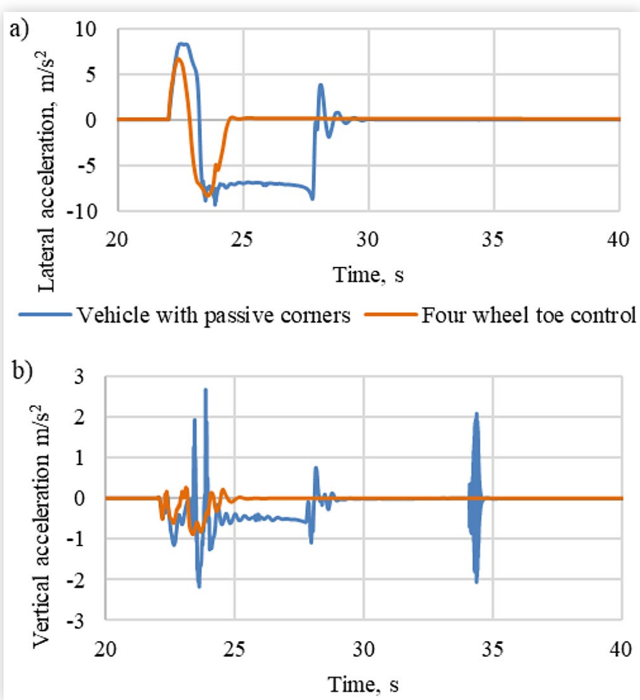

FIGURE 12 Accelerations achieved during double lane change: lateral (a) and vertical acceleration (b) of sprung mass

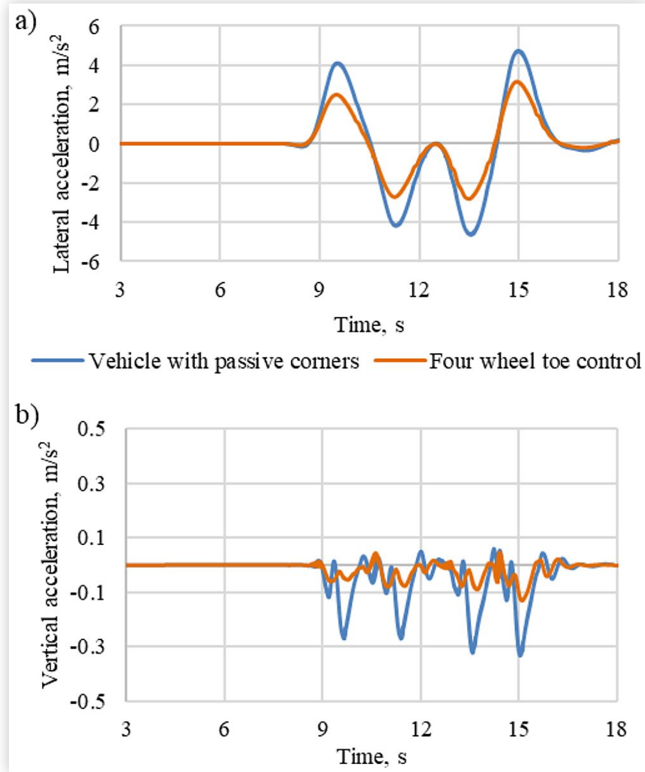

reduction. Similar analyses were conducted for the DLC maneuver, with results illustrated in Figure 12. Here, the RMS for vertical acceleration, within the time span from 9 to 18 seconds, underwent a significant change from 0.11 m/s^2 to 0.04 m/s^2, signifying a remarkable 63.4% decrease. It's important to note that literature typically provides difference thresholds for sinusoidal and random stimuli, which, under most adverse conditions, do not exceed 20% [10,11].

It's worth mentioning that acceleration measurements in this study consider the center of gravity of the vehicle, as opposed to the occupant's seating position, as is common in literature. However, the observed differences are substantial enough to indicate that occupants are likely to perceive the improvements. Consequently, it can be confidently asserted that the proposed active toe control system for vehicle corners not only enhances vehicle stability but also augments comfort levels. It is anticipated that the maximum impact of this technology will be realized with the development of an integrated chassis control system.

Conclusions

In this study, we introduced a novel vehicle corner architecture encompassing both the front and rear axles, with a particular focus on analyzing wheel positioning systems. Our findings reveal that the impact of active camber angle adjustment is constrained by tire geometry, resulting in only marginal increases in lateral force. Additionally, implementing such adjustments would require substantial actuator displacement, exceeding 200 mm for passenger cars, potentially leading to packaging challenges.

Conversely, toe angle adjustment yields a more substantial increase in tire lateral force and offers a wider range of adjustability. Importantly, integrating toe actuators into the vehicle's design does not necessitate complex modifications.

To enhance direct yaw rate control, we proposed the integration of toe actuators on both the front and rear axles. This approach can serve as a viable alternative to conventional dynamic control systems that rely on braking forces or be employed in conjunction with braking and propulsion systems. Achieved results indicate that the vehicle successfully executed maneuvers with the proposed control strategy, exhibiting minimal trajectory and velocity deviations. Furthermore, the implementation significantly reduced the yaw rate in both scenarios, contributing to improved vehicle performance and stability.

Notably, the active wheel positioning system led to reduced lateral and vertical accelerations during maneuvers. The notable decrease in the RMS of vertical acceleration surpasses the defined difference threshold, signifying a perceptible improvement in occupant comfort during extreme maneuvers.

References

1. Kojis, P., Danilevičius, A., Šabanovič, E., and Skrickij, V., *The Second Generation of Electric Vehicles: Integrated Corner Solutions* (Springer eBooks, 2022), 87-100. https://doi.org/10.1007/978-3-030-94774-3_9
2. Theunissen, J., Tota, A., Gruber, P., Dhaens, M. et al., "Preview-Based Techniques for Vehicle Suspension Control: A State-of-the-Art Review," *Annual Reviews in Control*, 51, 206-235, 2021. https://doi.org/10.1016/j.arcontrol.2021.03.010.
3. Förstberg, J., "Ride Comfort and Motion Sickness in Tilting Trains," PhD dissertation, Institutionen för farkostteknik, 2000. Retrieved from https://urn.kb.se/resolve?urn=urn:nbn:se:kth:diva-2985.
4. Chiari, A., Mantovani, S., Skrickij, V., and Boulay, E., "A Spline-Based Analytical Model for the Design of an Automotive Anti-Roll Bar," SAE Technical Paper 2023-01-0669 (2023). https://doi.org/10.4271/2023-01-0669.
5. Fujita, T., Fukao, T., Kinoshita, T., and Itagaki, N., "Semi-Active Suspension Improving both Ride Comfort and Handling Feel," *IFAC Proceedings Volumes* 46, no. 21 (2013): 225-230. https://doi.org/10.3182/20130904-4-jp-2042.00065.
6. Wang, K., Yang, M., Li, Y., Liu, Z. et al., "Multidirectional Motion Coupling Based Extreme Motion Control of Distributed Drive Autonomous Vehicle," *Scientific Reports* 12, no. 1 (2022). https://doi.org/10.1038/s41598-022-17351-4.
7. Jin, X., Wang, J., Yan, Z., Xu, L. et al., "Robust Vibration Control for Active Suspension System of in-Wheel-Motor-Driven Electric Vehicle Via μ-Synthesis Methodology. *Journal of Dynamic Systems Measurement and Control-Transactions of the Asme*, 144(5), 2022. https://doi.org/10.1115/1.4053661.
8. Jin, X., Wang, J., Sun, S., Li, S. et al., "Design of Constrained Robust Controller for Active Suspension of in-Wheel-Drive Electric Vehicles," *Mathematics* 9, no. 3 (2021): 249. https://doi.org/10.3390/math9030249.
9. Qin, Y., He, C., Ding, P., Dong, M. et al., "Suspension Hybrid Control for in-Wheel Motor Driven Electric Vehicle with Dynamic Vibration Absorbing Structures," *IFAC-PapersOnLine* 51, no. 31 (2018): 973-978. https://doi.org/10.1016/j.ifacol.2018.10.054.
10. Deubel, C., Ernst, S., and Prokop, G., "Objective Evaluation Methods of Vehicle Ride Comfort—A Literature Review," *Journal of Sound and Vibration*, 548, 117515, 2023. https://doi.org/10.1016/j.jsv.2022.117515.
11. Gräbe, R.P., Kat, C., Van Staden, P.J., and Schalk, P., "Difference Thresholds for a Vehicle on a 4-Poster Test Rig," *Applied Ergonomics* 87 (2020): 103115. https://doi.org/10.1016/j.apergo.2020.103115.
12. Anderson, M., and Harty, D., "Unsprung Mass with In-Wheel Motors – Myths and Realities," AVEC 10, the 10th International Symposium on Advanced Vehicle Control, published by Loughborough University, 2010, ISBN 0-9049-4765-3.
13. Žuraulis, V., Kojis, P., Marotta, R., Šukevičius, Š. et al., "Electric Vehicle Corner Architecture: Driving Comfort Evaluation Using Objective Metrics," SAE Technical Paper 2022-01-0921 (2022). https://doi.org/10.4271/2022-01-0921.
14. Milliken, W.F. and Milliken, D.L., *Race Car Vehicle Dynamics* (SAE International, 1994)
15. Jazar, R.N., *Vehicle Dynamics: Theory and Application*, (3rd ed.) ed. (Springer, 2017)
16. Abe, M., *Vehicle Handling Dynamics: Theory and Application*, (2nd ed.) ed. (Butter-worth-Heinemann, 2015)
17. Gao, J. and Wu, F., "Analysis and Optimisation of the Vehicle Handling Stability with Considering Suspension Kinematics and Compliance Characteristics," *Advances in Mechanical Engineering* 13, no. 5 (2021): 168781402110155. https://doi.org/10.1177/16878140211015523.
18. Sun, P., Trigell, A.S., Drugge, L., Jerrelind, J. et al., "Exploring the Potential of Camber Control to Improve Vehicles' Energy Efficiency during Cornering," *Energies* 11, no. 4: 724. https://doi.org/10.3390/en11040724.
19. Zhang, W., Drugge, L., Nybacka, M., and Wang, Z., "Active Camber for Enhancing Path Following and Yaw Stability of Overactuated Autonomous Electric Vehicles," *Vehicle System Dynamics* 59, no. 5 (2021): 800-821. https://doi.org/10.1080/00423114.2020.1723653.
20. Marotta, R., Strano, S., Terzo, M., Tordela, C. et al., "Active Control of Camber and Toe Angles to Improve Vehicle Ride Comfort," SAE Technical Paper 2022-01-0920 (2022). https://doi.org/10.4271/2022-01-0920.

21. Yu, C., Zheng, Y., Shyrokau, B., and Ivanov, V., "*MPC-Based Path Following Design for Automated Vehicles with Rear Wheel Steering*," IEEE International Conference on Mechatronics (ICM), Kashiwa, Japan, 2021, pp. 1-6, https://doi.org/10.1109/ICM46511.2021.9385606.
22. Roethof, D., Sezer, T., Arat, M., and Shyrokau, B., "Influence of Active Camber Control on Steering Feel," *SAE Int. J. Passeng. Cars - Mech. Syst.* 9, no. 1 (2016): 124-134. https://doi.org/10.4271/2016-01-0466.
23. Wright, K.R.S., Botha, T.R., and Schalk, P., "Effects of Age and Wear on the Stiffness and Friction Properties of an SUV Tyre," *Journal of Terramechanics* 84 (2019): 21-30. https://doi.org/10.1016/j.jterra.2019.04.001.
24. Park, K., Joa, E., Yi, K., and Yoon, Y., "Rear-Wheel Steering Control for Enhanced Steady-State and Transient Vehicle Handling Characteristics," *IEEE Access* 8 (2020): 149282-149300. https://doi.org/10.1109/access.2020.3014719.
25. Shyrokau, B. and Wang, D.. "Control Allocation with Dynamic Weight Scheduling for Two-Task Integrated Vehicle Control," In *Proc. 11th Int. Symp. Adv. Vehicle Control*, pp. 1-6, 2012.
26. Šabanovič, E., Žuraulis, V., Prentkovskis, O., and Skrickij, V., "Identification of Road-Surface Type Using Deep Neural Networks for Friction Coefficient Estimation," *Sensors* 20, no. 3 (2020): 612. https://doi.org/10.3390/s20030612.
27. Vaseur, C., and Van Aalst, S., "Test Results at Ford Lommel Proving Ground ESR 11," (Final) [Data set], 2019, Zenodo. https://doi.org/10.5281/zenodo.3263811.

Acknowledgments

This work was supported by the Research Council of Lithuania project no. S-MIP-23-120.

Definitions/Abbreviations

EV - electric vehicle
IWM - in-wheel motor
DT - difference threshold
MPC - model predictive control
DLC - double lane change
PID - Proportional integral derivative controller
RMS - Root mean square
CAD - Computer-aided design
SUV - Sport utility vehicle
DSC - Dynamic Stability Control
COG - Centre of gravity position

ISSN 0148-7191